JOC The Journal of Organic Chemistry

NOTE

pubs.acs.org/joc

N-1- and *N*-2-Anthryl Succinimide Derivatives: C−N Bond Rotational Behaviors and Fluorescence Energy Transfer

Teh-Chang Chou,*[,†] Ren-Tsung Wu,[†] Kung-Ching Liao,[‡] and Chun-Hung Wang[‡]

[†]Department of Applied Chemistry, Chaoyang University of Technology, Wufong, Taichung, 41369, Taiwan

[‡]Institute of Chemistry, Academia Sinica, No. 128, Sec. 2, Academia Road, Taipei 115, Taiwan

Supporting Information

ABSTRACT: New rigid bicyclic *N*-anthrylsuccinimide **1a**, **1b**, **2a**, and **2b** were prepared. The $C_{aryl}-N_{imide}$ bond rotational barriers, intra/intermolecular arene−arene interactions, and photophysical properties were investigated. The rotational behaviors are more significantly controlled by the position of $C_{aryl}-N_{imide}$ connection than the sidewall framework. The fluorescence energy transfer (Φ_{ET}) in **1a** and **1b** was estimated to be 61% and 53%, respectively. The difference is attributed to the position of $C_{aryl}-N_{imide}$ connection, which directly influences the relative orientation of donor (naphthalene) and acceptor (anthracene).

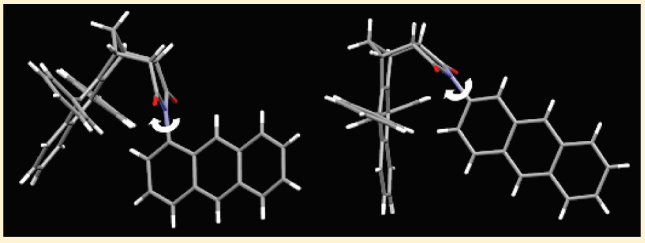

Recently, investigations toward a better understanding of weak noncovalent interactions involving aromatic rings has led to design small molecular systems featuring rigid polycyclic *N*-arylsuccinimide scaffolds, taking advantage of their concave molecular geometry that can fasten the *N*-aryl substituent closely interacting with the sidewall arene moiety.[1−12] The arene−arene interactions between aryl sidewall and *N*-aryl moiety could subsequently affect molecular properties, such as the conformational preferences,[1−5] molecular packing motifs in solid states,[6,7] and intramolecular charge/energy transfer,[8−10] granting opportunity to scrutinize the intra/intermolecular $\pi\cdots\pi$ (face-to-face) and $CH\cdots\pi$ (edge-to-face) interactions.[11,12] In this context, we designed and prepared rigid bicyclic *N*-anthrylsuccinimides **1a**, **1b**, **2a**, and **2b** (shown in Scheme 1). These succinimides are characterized by two structural features, the presence or absence of diphenylnaphthalene sidewall (**1a** vs **2a** and **1b** vs **2b**) and the attachment position of N_{imide} to anthracene ring (**1a** vs **1b** and **2a** vs **2b**). The effects of these features were evaluated by the intra/intermolecular arene−arene interactions relating to the rotational behaviors of *N*-anthryl ring about $C_{aryl}-N_{imide}$ bond, the molecular packing in the solid state, and photophysical properties. Herein, we report the results.

As shown in Scheme 1, the synthesis of *N*-anthrylsuccinimides **1a**, **1b**, **2a**, and **2b** started from the Diels−Alder reaction of bicyclo[2.2.1]hept-5-ene-2,3-dicarboxylic anhydride (**3**)[13] and 1,3-diphenylisobenzofuran (**4**), followed by the acid-catalyzed dehydration (aromatization) of the resulting adduct **5** (without isolation) to give diphenylnaphthalene-fused bicyclic anhydride **6** (overall yield 77%). The condensation reaction of **6** with 1-aminoanthracene (**7a**) or 2-aminoanthracene (**7b**) was then carried out in refluxing acetic acid, catalyzed by $Zn(OAc)_2$,[8,13] to afford the corresponding *N*-anthrylsuccinimides **1a** (96%) and **1b** (90%). Similar condensation reactions of anhydride **3** with **7a** or **7b** furnished *N*-anthrylsuccinimides **2a** (90%) and **2b** (91%), respectively. All the newly synthesized *N*-anthrylsuccinimides (**1a**,**b** and **2a**,**b**) were fully characterized (see Experimental Section) and further unequivocally established via the X-ray crystallographic analysis (vide infra).

Because of the steric interaction of the *N*-aryl hydrogens with the imide carbonyl groups, the aryl group is prevented from being coplanar with the plane of succinimide ring, resulting in affecting the effectiveness of electron delocalization of the unshared electron pair on the nitrogen atom to the aryl ring, as well as the rotation about the single bond that joins the aryl ring to the nitrogen atom. The restricted rotation of the *N*-anthryl ring about $C_{aryl}-N_{imide}$ bond in **1a**/**1b** (and **2a**/**2b**) would give rise to two distinct stereoisomers having unfolded-conformation (exo-) and folded-conformation (endo-), designated by the relative orientation (syn or anti) between the naphthalenyl moiety bearing C-9 and the methano-bridge, as depicted in Figure 1. The $C_{aryl}-N_{imide}$ bond rotational barriers are expected to be influenced by the attachment position of anthryl carbon (C-1 or C-2) to the nitrogen atom of succinimide ring and the presence of aryl sidewall. We thus embarked on investigating the rotational barriers of **1** and **2** by using ^{1}H NMR spectroscopy and computational methods.

The assignments of the absorption signals for the protons were made using intensity, chemical shift, and splitting pattern, and further supported by COSY experiments (Figures S1−S10, Supporting Informations, SI). When crystalline *N*-(1-anthryl)-succinimides **1a** and **2a** were, respectively, dissolved in cold

Received: April 13, 2011
Published: July 05, 2011

Scheme 1

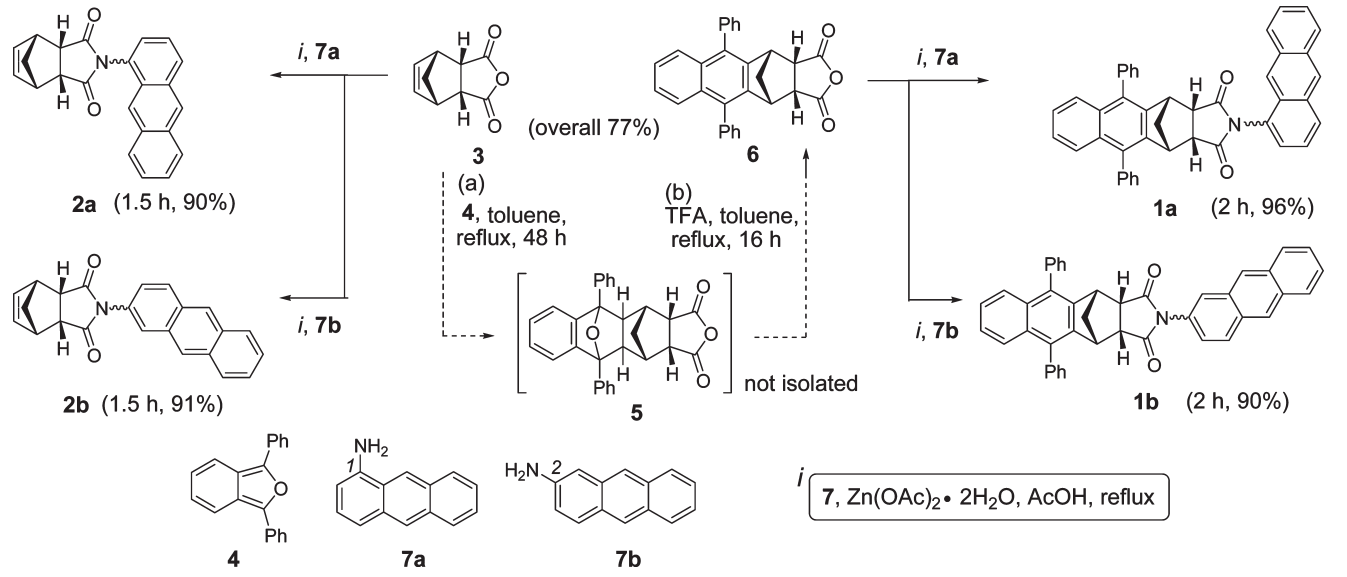

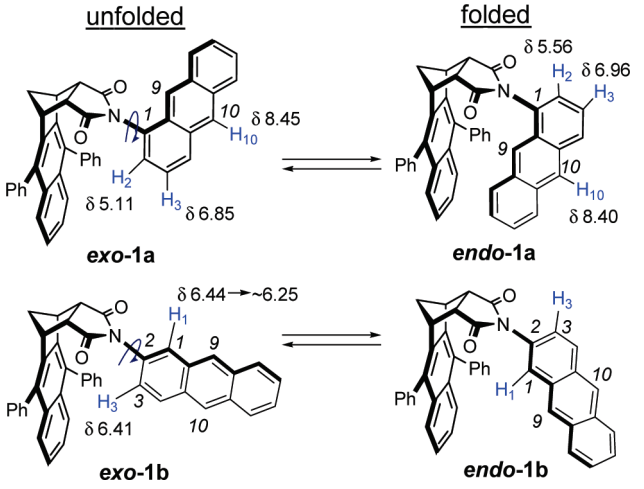

Figure 1. Two conformations, *exo*- and *endo*-, of **1a** and **1b**, resulting from restricted rotation about the *N*-aryl single bond. The chemical shift (δ) for H-1 of **1b** changed from 6.44 at 303 K to about 6.25 at 213 K, while that of H-3 remained unchanged.

CD_2Cl_2 (ca. −20 °C) and immediately examined in a NMR spectrometer at 253 K, the ^{1}H NMR spectra indicated that they existed predominately in one conformer (Figures S2a/S4a in SI). They were assigned, respectively, the exo-conformers, *exo*-**1a** and *exo*-**2a**, as depicted in Figure 1, suggested by their solid-state structures (vide infra) and the relatively upfield located signals for anthryl H-2 (**1a**, δ 5.11; **2a**, δ 7.13) and H-3 (**1a**, δ 6.85) due to anisotropic shielding by the sidewall aromatic rings or C═C bond.[14,15] The ^{1}H NMR spectra of **1a** and **2a** were then recorded at a constant temperature (308 K) at regular time intervals (5 min) until the rotational process attained an equilibrium.

As shown in Figure S12 in SI, a new set of absorption signals emerged and augmented in each spectrum of **1a**, which was attributed to the appearance of other conformer, the *endo*-**1a**. The equilibration ^{1}H NMR spectra of **2a** behaved similarly (Figure S13 in SI). As noted in Figure 1, the anthryl H-2 (δ 5.56) and H-3 (δ 6.96) of *endo*-**1a** were found to display absorption signals at lower magnetic field as compared with the respective protons of *exo*-**1a**, because they swung away from the shielding zone of the sidewall aromatic rings. Meanwhile, the anthryl H-10 moved into the shielding zone, showing signal at higher field for *endo*-**1a** (δ 8.40) relative to that for *exo*-**1a** (δ 8.45). The results of ^{1}H NMR equilibration study led us to attain the time-dependent ratios of exo- and endo-conformers and therefore the rotational barriers of C_{aryl}—N_{imide} bond for **1a** and **2a** calculated according to the equations introduced by Shimizu et al.[1,2,16] The rotational barriers for **1a** and **2a** were approximately 92.0 and 91.1 kJ/mol, respectively, which were supported by the results of theoretical calculations (vide infra). At equilibrium (308 K), the exo/endo ratios of compounds **1a** and **2a** were observed to be 65:35 and 55:45, respectively, implying that the unfolded exo-conformation is more stable than the folded endo-conformation. The higher rotational barrier and the bigger difference in population of exo/endo conformers for **1a** than for **2a** may be ascribed to the larger steric hindrance between the 1-anthryl group and the diphenylnaphthalene sidewall.

On the contrary, the room-temperature ^{1}H NMR spectra of *N*-(2-anthryl)succinimides **1b** and **2b**, which remained unchanged over time, showed signals ascribable to either exo- or endo-conformer or rapidly interconverting conformers. The diphenylnaphthalene-fused **1b** was further investigated using the variable-temperature ^{1}H NMR technique.[3,16] As shown in Figure S14 in SI, the C_{aryl}—N_{imide} bond rotation was still rapid and basically similar pattern of absorption signals was observed even at temperature lowered to 183 K. The observed chemical shifts were due to the "averaged" peaks. One signal worthy of notice is the one-proton singlet at δ 6.44 due to the anthryl H-1 (see Figure 1), which broadened and moved upfield significantly with decreasing temperature, and finally flattened out at 183 K together with one-proton doublet at δ 6.41 (H-3).

We adopted the PCM/MP2/6-31G(d)//B3LYP/6-31G(d) approximation to calculate the C_{aryl}—N_{imide} bond rotational barrier in CH_2Cl_2 for each *N*-anthrylsuccinimide (Figures S15 and S16 in SI).[3,17] For *N*-(1-anthryl)succinimides **1a** and **2a**, the

dx.doi.org/10.1021/jo200665v |*J. Org. Chem.* 2011, 76, 6813–6818

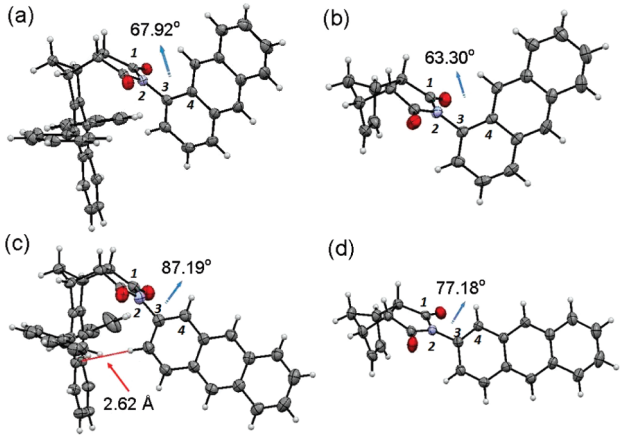

Figure 2. ORTEP drawings of *N*-anthrylsuccinimides: (a) **1a**, (b) **2a**, (c) **1b**, and (d) **2b**. The arrows indicate the succinimide−anthracene dihedral angles defined by C1−N2−C3−C4.

Scheme 2

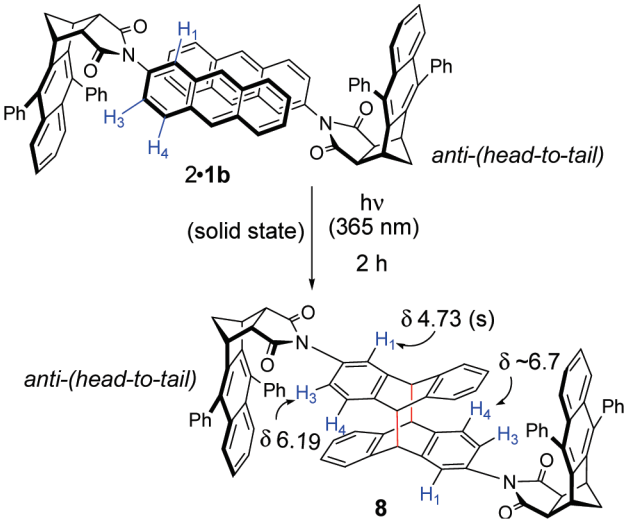

rotational barriers were estimated to be 98.6 and 85.8 kJ/mol, respectively, comparable to the values derived from ^{1}H NMR equilibration study. On the other hand, the rotational barriers for *N*-(2-anthryl)succinimides **1b** and **2b** were calculated to be 26.5 and 22.8 kJ/mol, respectively, in line with the results observed in the variable-temperature ^{1}H NMR spectra of **1b**. On the basis of the estimated rotational barriers, the $C_{aryl}-N_{imide}$ bond rotational rates of **1b** and **2b** are extremely rapid, and the half-lives for their rotational motion are about 2.5 ns and 0.55 ns at 298 K, respectively. However, the $C_{aryl}-N_{imide}$ bond rotational behaviors of **1a** and **2a** are more restricted and relatively slower, and the time scales for their half-lives are about 12.6 min and 8.6 min at 298 K, respectively.[1] The results from calculations have also shown that $C_{aryl}-N_{imide}$ bond rotational behaviors are more influenced by the position of N_{imide} attachment due to the steric hindrance between succinimide carbonyl groups and *N*-anthryl ring.

The solid-state structures of *N*-anthrylsuccinimides (**1a**,**b** and **2a**,**b**) are shown in Figure 2. The crystal structures of **1a** and **2a** displayed similar exo-conformation with the succinimide−anthracene dihedral angles measured to be 67.92° and 63.30°, respectively (Figure 2a,b).[11] No significant intramolecular interaction between the anthryl ring and the sidewall aromatic rings or C=C bond was observed in the crystal structures of **1a** and **2a**. On the other hand, probably due to the consequence of additional steric interaction between the *N*-aryl hydrogen (H-1 and H-3) and the imide carbonyl groups, the succinimide−anthracene dihedral angles in **1b** and **2b** were found to be larger, amounting to 87.19° and 77.18°, respectively (Figure 2c,d). In the crystal structure of **1b** (Figure 2c), the anthryl ring is located in close proximity to the diphenylnaphthalene sidewall suitable for H-3 of anthracene ring to exert an attractive intramolecular CH$\cdots\pi$ (edge-to-face) interaction with aromatic sidewall ($d_{H\cdots\pi}$ = 2.62 Å).[18−21] Consequently, the plane of anthracene ring in *exo*-**1b** is oriented nearly perpendicular to succinimide ring with a succinimide−anthracene dihedral angle larger than that of **2b**, which lacks an intramolecular CH$\cdots\pi$ interaction (Figure 2d).

Probably as a consequence of distinct sidewall structure and varied orientation of the anthryl ring resulting from different position of anthryl carbon (C-1 vs C-2) linked to N_{imide}, the *N*-anthrylsuccinimides displayed dissimilar crystal packing motifs for the "dimeric" structure. The crystal packing motifs for the dimeric structures of **1a**,**b** and **2a**,**b** are shown in Figure S17 in SI. A weak intermolecular $\pi\cdots\pi$ interaction (interplanar distance 3.5 Å, centroid-to-centroid distance 6.08 Å) and an intermolecular CH$\cdots\pi$ interaction between anthracene rings ($d_{H\cdots\pi}$ = 2.78 Å) were observed for **2a** and **2b**, respectively (Figure S18c,d in SI). In contrast, the dimeric structure of **1a** is realized by the CH$\cdots\pi$ (edge-to-face) interaction[17−21] between anthracene ring of one molecule of **1a** and phenyl ring of another ($d_{H\cdots\pi}$ = 2.95 Å), Figure S17a in SI. However, as shown in Figure S17b in SI, two molecules of **1b** align in *N*-style, having their anthracene rings to perform an effective intermolecular $\pi\cdots\pi$ (face-to-face) interaction with an interplanar distance of 3.5 Å and a centroid-to-centroid distance of 3.82 Å. It is worthy to note that intermolecular close contacts with distances of about 2.5 Å between the C=O of the succinimide ring and the aryl hydrogen were found to reinforce the crystal packing motifs of **1a**, **1b**, and **2a**.

The anti-(head-to-tail), $\pi\cdots\pi$ stacking motif of **1b** (Figure S17b in SI) prompted us to investigate its solid-state photochemical behavior.[22,23] Thus, when yellow crystals of **1b** were pulverized and irradiated using 365 nm-light for 2 h, the reaction yielded a photodimeric product as pale brown powders of low solubility. The assignment of anti-(head-to-tail)-structure **8** to the product (Scheme 2), rather than the syn-(head-to-tail)-structure, was suggested by the $\pi\cdots\pi$ stacking motif of monomer **1b**, and supported by the ^{1}H NMR spectrum (Figure S8 in SI), H−H COSY (Figure S11 in SI), and the similarity of solid-state UV absorption and emission spectra to those of anhydride **6** (Figure S18 in SI).[24]

The UV spectra of *N*-anthrylsuccinimides (**1a**,**b** and **2a**,**b**) and succinic anhydride **6** in $CHCl_3$ (Figure S19 in SI) contain major bands in the regions of 240−280, 280−310, and 330−390 nm, characteristic of diphenylnaphthalene and anthracene chromophores. Figure 3a,b shows the emission spectra under excitation at wavelengths of either 295 or 365 nm.[25] The fundamental UV absorption and fluorescence properties are summarized in Table S5 in SI. As shown in Figure 3a, the fluorescence spectra of all *N*-anthrylsuccinimides are identical in shape, suggesting

dx.doi.org/10.1021/jo200665v |*J. Org. Chem.* 2011, 76, 6813–6818

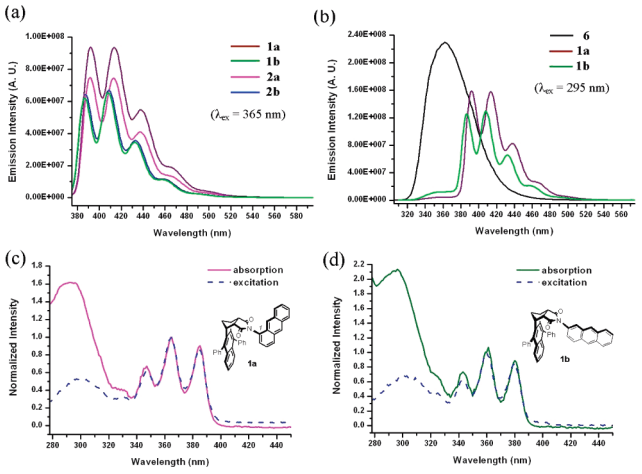

Figure 3. Emission spectra (2×10^{-5} M in $CHCl_3$) of *N*-anthrylsuccinimides: (a) excited at λ_{ex} 365 nm, and (b) **1a**, **1b**, and succinic anhydride **6** excited at λ_{ex} 295 nm. Fluorescence excitation (dash line) spectra in $CHCl_3$ normalized to match the absorption spectra (solid line) in the anthracene region: (c) **1a** (measured at 467 nm) and (d) **1b** (measured at 460 nm).

that the two spaced diphenylnaphthalene and anthracene chromophores in **1a** and **1b** are essentially independent of each other.[26,27] However, as evidently shown by Figure 3b, succinimides **1a** and **1b** displayed intramolecular energy transfer phenomena from diphenylnaphthalene to anthracene chromophores.[28,29]

The quantum efficiencies (Φ_{ET}) of intramolecular energy transfer for **1a** and **1b** are estimated using the comparison of the absorption spectra and corresponding fluorescence excitation spectra (Figure S20 in SI). Because the naphthalene emission least affected the emission wavelengths of 467 and 460 nm based in Figure 3b, the fluorescence excitation profiles for **1a** and **1b** measured respectively at these two wavelengths were normalized to best match the absorption spectra in the anthracene region (330−390 nm) as shown in Figures 3c,d. The values of Φ_{ET}, defined as the ratio of the areas under the normalized excitation and absorption curves, are calculated to be 61% and 53% for **1a** and **1b**, respectively.[29] The difference in energy transfer efficiency in **1a** and **1b** may be attributed to the differences in the distance, the relative orientation, and the HOMO energy level between the acceptor (anthracene) and donor (diphenylnaphthalene) chromophores,[26] and the ratios of folded and unfolded conformations, all of which are directly related to the attachment position of N_{imide} to anthracene (C-1 vs C-2). The results suggest that the *N*-1-anthryl group can serve as a more efficient energy acceptor than the *N*-2-anthryl group.

In conclusion, a series of rigid bicyclic *N*-anthrylsuccinimide **1a**, **1b**, **2a**, and **2b** were prepared. The $C_{aryl}-N_{imide}$ bond rotational barriers of *N*-(1-anthryl)succinimide **1a** and **2a** are considerably larger than those of *N*-(2-anthryl)succinimide **1b** and **2b**. The results have shown that the rotational behaviors and conformational preference are more significantly controlled by the position of $C_{aryl}-N_{imide}$ connection (the steric effect of *N*-anthryl and two carbonyl groups) than the sidewall framework. The intramolecular naphthalene-to-anthracene fluorescence energy transfer was observed in **1a** and **1b**. The values of energy transfer efficiency (Φ_{ET}) were estimated to be 61% and 53% for **1a** and **1b**, respectively. The difference in Φ_{ET} may be attributed to the position of $C_{aryl}-N_{imide}$ connection, which directly influences the relative orientation of donor (naphthalene) and acceptor (anthracene).

EXPERIMENTAL SECTION

Diphenylnaphthalene-Fused Bicyclic Anhydride (6). A solution of *cis-endo*-bicyclo[2.2.1]hept- 5-ene-2,3-dicarboxylic anhydride (**3**)[13] (0.821 g, 5.0 mmol), and 1,3-diphenylisobenzofuran (**4**) (1.35 g, 5 mmol) in toluene (15 mL) was refluxed for 48 h.[9] After completion of Diels−Alder cycloaddition, the reaction mixture was cooled to room temperature, treated with trifluoroacetic acid (1.7 mL, 22 mmol), and then heated under refluxing with a Dean−Stark trap for 16 h.[12] The reaction mixture was washed by 1.0 M $NaHCO_3$ aqueous solution (5 mL × 3), and the aqueous solution was extracted with CH_2Cl_2 (10 mL × 3). The combined organic layers were dried over anhydrous $MgSO_4$, filtered, and evaporated into dryness to afford a white powder (1.60 g, 77%) of **6**: mp 281−283 °C ($CHCl_3$/EtOH); ^{1}H NMR (CD_2Cl_2, 400 MHz, 298 K): δ 7.63−7.45 (m, 10H), 7.45−7.33 (m, 4H), 3.97 (s, 2H), 3.72 (s, 2H), 2.27 (d, J = 12 Hz, 1H), 1.99 (d, J = 12 Hz, 1H) ppm; ^{13}C NMR ($CDCl_3$, 100 MHz, 298 K): δ 170.2 (C), 136.2 (C), 134.3 (C), 132.5 (C), 131.2 (CH), 130.0 (CH), 128.3 (CH), 128.2 (CH), 127.7 (CH), 126.7 (CH), 126.0 (CH), 52.0 (CH_2), 49.1 (CH), 46.0 (CH) ppm; MS (FAB) m/z 416.1 $[M]^+$, 100%; HRMS (FAB) calcd for $C_{29}H_{20}O_3$ 416.1412; obsd m/z 416.1404 $[M]^+$. Anal. Calcd for $C_{29}H_{20}O_3$: C, 83.63; H, 4.84. Found: C, 83.79; H, 4.85.

Diphenylnaphthalene-Fused *N*-(1-Anthryl)succinimide (1a). To a solution of bicyclic anhydride **6** (0.345 g, 0.83 mmol) and 1-aminoanthracene (0.160 g, 0.83 mmol) in acetic acid (6 mL) was added zinc acetate dihydrate (0.018 g, 0.08 mmol). The reaction mixture was refluxed for 2 h. After cooling, the reaction mixture was poured into ice−water (120 mL). The aqueous solution was extracted with CH_2Cl_2 (20 mL × 3), and the organic layers were combined and washed with 0.5 M $NaHCO_3$ aqueous solution (20 mL × 3). The organic layer was dried over anhydrous $MgSO_4$, filtered, and evaporated into dryness to afford a dark brown solid. The crude product was chromatographed on silica gel (CH_2Cl_2/Et_2O = 10:1) yielding **1a** as a yellow solid (0.468 g, 96%): mp >350 °C ($CHCl_3$/EtOH); ^{1}H NMR (CD_2Cl_2, 500 MHz, 257 K): δ 8.45 (s, 1H), 7.99−7.92 (m, 4H), 7.67−7.66 (m, 2H), 7.55−7.43 (m, 12H), 7.26 (d, J = 5 Hz, 2H), 6.87−6.84 (m, 1H), 5.11 (d, J = 5 Hz, 1H), 4.06 (s, 2H), 3.82 (s, 2H), 2.38 (d, J = 10 Hz, 1H), 2.14 (d, J = 10 Hz, 1H) ppm; ^{13}C NMR (CD_2Cl_2, 100 MHz, 298 K): δ 176.3 (C), 175.9 (C), 139.5 (C), 138.4 (C), 137.4 (C), 137.3 (C), 134.5 (C), 134.1 (C), 132.7 (C), 132.3 (C), 132.1 (C), 131.9 (C), 131.4 (CH), 131.1 (CH), 130.5 (CH), 130.1 (CH), 130.1 (CH), 129.9 (CH), 128.9 (C), 128.6 (CH), 128.3 (CH), 128.2 (CH), 128.0 (CH), 127.9 (CH), 127.5 (CH), 127.4 (CH), 127.2 (CH), 127.1 (CH), 126.7 (CH), 126.1 (CH), 126.0 (CH), 125.8 (CH), 125.6 (CH) 125.0 (CH), 124.1 (CH), 120.7 (CH), 120.1 (CH), 54.2 (CH_2), 51.5 (CH_2), 49.1 (CH), 48.5 (CH), 45.8 (CH), 45.4 (CH) ppm; MS (FAB): m/z 592.2 $[M + H]^+$, 100%; 591.2 $[M]^+$, 90%; HRMS (FAB) calcd for $C_{43}H_{30}NO_2$: 592.2271; obsd m/z 592.2280 $[M + H]^+$. Anal. Calcd for $C_{43}H_{29}NO_2$: C, 87.28; H, 4.94; N, 2.37. Found: C, 87.32; H, 4.74; N, 2.13.

Diphenylnaphthalene-Fused *N*-(2-Anthryl) Succinimide (1b). To a solution of bicyclic anhydride **6** (0.345 g, 0.83 mmol) and 2-aminoanthracene (0.160 g, 0.83 mmol) in acetic acid (6 mL) was added zinc acetate dihydrate (0.018 g, 0.08 mmol). The reaction mixture was refluxed for 2 h. After cooling, the reaction mixture was poured into ice−water (120 mL). The aqueous solution was extracted with CH_2Cl_2 (20 mL × 3), and the organic layers were combined and washed with 0.5 M $NaHCO_3$ aqueous solution (20 mL × 3). The organic layer was dried over anhydrous $MgSO_4$, filtered, and evaporated into dryness to afford a pale brown solid. The crude product was chromatographed on silica gel (EtOAc/*n*-Hex = 1:2, and then CH_2Cl_2/Et_2O = 10:1) yielding the **1b** as a yellow solid (0.442 g, 90%): mp 340−342 °C ($CHCl_3$/EtOH).

dx.doi.org/10.1021/jo200665v |*J. Org. Chem.* 2011, 76, 6813–6818

^{1}H NMR (CD_2Cl_2, 400 MHz, 298 K): δ 8.35 (s, 1H), 7.99−7.96 (m, 1H), 7.90−7.88 (m, 1H), 7.78 (d, J = 8 Hz, 1H), 7.74−7.69 (m, 3H), 7.55−7.31 (m, 14H), 6.44−641 (m, 2H), 4.03 (s, 2H), 3.63 (s, 2H), 2.36 (d, J = 8 Hz, 1H), 2.09 (d, J = 8 Hz, 1H) ppm; ^{13}C NMR ($CDCl_3$, 100 MHz, 298 K): δ 175.8 (C), 138.4 (C), 137.3 (C), 134.1 (C), 132.5 (C), 132.1 (C), 131.7 (C), 131.4 (CH), 130.7 (C), 130.2 (CH), 129.5 (CH), 128.7 (C), 128.2 (CH), 128.1 (CH), 127.6 (CH), 126.8 (CH), 126.7 (CH), 126.1 (CH), 125.8 (CH), 125.8 (CH), 125.7 (CH), 123.8 (CH), 51.1 (CH_2), 48.2 (CH), 45.8 (CH) ppm; MS (FAB): m/z 592.2 $[M + H]^+$, 100%; 540.4, 48%; HRMS (FAB) calcd for $C_{43}H_{30}O_2N$: 592.2277; obsd m/z 592.2283 $[M + H]^+$. Anal. Calcd for $C_{43}H_{29}NO_2$: C, 87.28; H, 4.94; N, 2.37. Found: C, 87.35; H, 4.57; N, 2.29.

***N*-(1-Anthryl) Succinimide (2a).** To a solution of *cis-endo*-bicyclo[2.2.1]hept-5-ene-2,3- dicarboxylic anhydride (**3**)[13] (0.136 g, 0.83 mmol) and 1-aminoanthracene (0.160 g, 0.83 mmol) in acetic acid (6 mL) was added zinc acetate dihydrate (0.018 g, 0.08 mmol). The reaction mixture was refluxed for 2 h. After cooling, the reaction mixture was poured into ice−water (120 mL) and was extracted with CH_2Cl_2 (20 mL × 3). The organic layers were combined and washed with 0.5 M $NaHCO_3$ aqueous solution (20 mL × 3), dried over anhydrous anhydrous $MgSO_4$, filtered, and evaporated into dryness to afford a dark brown solid. The crude product was further purified by column chromatography on silica gel (CH_2Cl_2) giving **1b** as a pale brown solid (0.254 g, 90%): mp 227−228 °C ($CHCl_3$/EtOH); ^{1}H NMR (CD_2Cl_2, 500 MHz, 253 K): δ 8.54 (s, 1H), 8.13−8.11 (m, 3H), 8.05−7.98 (m, 2H), 7.52−7.48 (m, 3H), 7.13 (d, J = 5 Hz, 1H), 6.39 (s, 2H), 3.71 (s, 2H), 3.55 (s, 2H), 1.82 (d, J = 10 Hz, 1H), 1.71 (d, J = 10 Hz, 1H) ppm; ^{13}C NMR ($CDCl_3$, 100 MHz, 298 K): δ 177.3 (C), 177.0 (C), 136.1 (CH), 134.8 (CH), 132.2 (C), 132.1 (C), 132.0 (C), 131.9 (C), 130.3 (CH), 129.4, 129.0, 128.4 (CH), 128.3 (CH), 128.1 (CH), 127.5, 127.5, 127.4 (CH), 127.2 (CH), 126.3 (CH), 126.0 (CH), 125.9 (CH), 125.8 (CH), 124.4 (CH), 124.3 (CH), 121.8 (CH), 120.7 (CH), 53.0 (CH_2), 52.4 (CH_2), 47.1 (CH), 46.1 (CH), 45.7 (CH), 45.4 (CH) ppm; MS (FAB+): m/z 340.1 ($M+H^+$, 90%), 339.1 (M^+, 100%), 307.1 (43%); MS (FAB): m/z 340.1 $[M + H]^+$, 90%; 339.1 $[M]^+$, 100%; 307.1, 43%; HRMS (FAB) calcd for $C_{23}H_{17}NO_2$: 339.1259; obsd m/z 339.1259 $[M]^+$. Anal. Calcd for $C_{23}H_{17}NO_2$: C, 81.40; H, 5.05; N, 4.13. Found: C, 81.25; H, 5.06; N 4.05.

***N*-(2-Anthryl) Succinimide (2b).** To a solution of *cis-endo*-bicyclo[2.2.1]hept-5-ene-2,3- dicarboxylic anhydride (**3**)[13] (0.136 g, 0.83 mmol) and 2-aminoanthracene (0.160 g, 0.83 mmol) in acetic acid (6 mL) was added zinc acetate dihydrate (0.018 g, 0.08 mmol). The reaction mixture was refluxed for 1.5 h. After cooling, the reaction mixture was poured into ice−water (120 mL). The aqueous solution was extracted with CH_2Cl_2 (20 mL × 3), and the organic layers were combined and washed with 0.5 M $NaHCO_3$ aqueous solution (20 mL × 3). The organic layer was dried over anhydrous $MgSO_4$, filtered, and evaporated into dryness to afford a brown solid. The crude product was further purified by column chromatography on silica gel (CH_2Cl_2) giving a pale brown solid of **2b** (0.256 g, 91%): mp 218−220 °C (CH_2Cl_2/EtOH); ^{1}H NMR (CD_2Cl_2, 400 MHz, 298 K): δ 8.47 (d, J = 8 Hz, 2H), 8.07−8.03 (m, 3H), 7.81 (s, 1H), 7.52−7.51 (m, 2H), 7.19 (d, J = 8 Hz, 1H), 6.34 (s, 2H), 3.50 (s, 4H), 2.36 (d, J = 8 Hz, 1H), 2.09 (d, J = 8 Hz, 1H) ppm; ^{13}C NMR ($CDCl_3$, 100 MHz, 298 K): δ 176.9 (C), 134.7 (CH), 132.2 (C), 131.9 (C), 130.9 (C), 130.7 (C), 129.4 (CH), 128.8 (C), 128.2 (CH), 128.2 (CH), 126.9 (CH), 126.3 (CH), 125.9 (CH), 125.8 (CH), 125.8 (CH), 123.7 (CH), 52.3 (CH_2), 45.9 (CH), 45.6 (CH) ppm; MS (FAB): m/z 339.1 $[M]^+$, 100%; 307.1, 88%; HRMS (FAB) calcd for $C_{23}H_{17}NO_2$: 339.1259; obsd 339.1264 $[M]^+$. Anal. Calcd for $C_{23}H_{17}NO_2$: C, 81.40; H, 5.05; N, 4.13. Found: C, 81.12; H, 5.07; N, 4.19.

Photodimerization of 1b, Formation of Dimer (8). The pulverized crystalline of *N*-2-anthrylimide **1b** was sandwiched in two glass plates, and then was irradiated in a Rayonet photochemical reactor with wavelength of 365 nm for 2 h. The reaction gave a brown product quantitatively, which displayed low solubility in most ordinary NMR solvents: mp 335−337 °C. ^{1}H NMR ($CDCl_3$, 400 MHz, 25 °C): δ 7.82−7.73 (m, 4H), 7.62−7.31 (m, 24H), 6.86−6.82 (m, 4H), 6.64−6.61 (m, 4H), 6.42 (d, J = 8 Hz, 2H), 6.16 (d, J = 8 Hz, 2H), 4.73 (s, 2H), 3.93−3.86 (m, 6H), 3.47−3.44 (m, 4H), 3.37 (d, J = 12 Hz, 2H), 2.25 (d, J = 12 Hz, 2H), 1.97 (d, J = 12 Hz, 2H) ppm; MS (FAB): m/z 1183.45 $[M + H]^+$, 100%; HRMS (FAB) calcd for $C_{86}H_{59}N_2O_4$: 1183.4469; obsd m/z 1183.4478 $[M + H]^+$.

■ ASSOCIATED CONTENT

Supporting Information. The proton and carbon NMR spectra of **1**, **2**, **6**, and **8**; proton−proton COSY spectra of **1a**, **2a**, and **8**; ^{1}H NMR equilibration spectra of **1a** and **2a**; variable-temperature ^{1}H NMR spectra of **1b**; the potential energy curves of the C−N bond rotational barriers; ORTEP drawings of *N*-anthrylsuccinimides; crystal data/structure refinement for **1a**, **2b**, **2a**, and **2b** (with cif files); the UV spectra of **1a**, **2b**, **2a**, **2b**, and **6**; the table of UV absorption and fluorescence properties; the solid-state absorption and emission spectra of dimer **8**; ^{1}H NMR spectra of compound **1b** and its photoadduct **8**. This material is available free of charge via the Internet at http://pubs.acs.org.

■ AUTHOR INFORMATION

Corresponding Author
*E-mail: tcchou@cyut.edu.tw.

■ ACKNOWLEDGMENT

This work was supported by a Theme Project from the Institute of Chemistry, Academia Sinica, Taiwan.

■ REFERENCES

(1) Rushton, G. T.; Burns, W. G.; Lavin, J. M.; Chong, Y. S.; Pellechia, P.; Shimizu, K. D. *J. Chem. Educ.* **2007**, *84*, 1499–1501.
(2) Chong, Y. S.; Carroll, W. R.; Burns, W. G.; Smith, M. D.; Shimizu, K. D. *Chem.—Eur. J.* **2009**, *15*, 9117–9126.
(3) Tafazzoli, M.; Ziyaei-Halimjani, A.; Ghiasi, M.; Fattahi, M.; Saidi, M. R. *J. Mol. Struct.* **2008**, *886*, 24–31.
(4) Kishikawa, K.; Yoshizaki, K.; Kohmoto, S.; Yamamoto, M.; Yamaguchi, K.; Yamada, K. *J. Chem. Soc., Perkin Trans. 1* **1997**, 1233–1239.
(5) Marshall, K.; Rosmarion, K.; Sklyut, O.; Azar, N.; Callahan, R.; Rothchild, R. *J. Fluorine Chem.* **2004**, *125*, 1893–1907.
(6) Eto, M.; Setoguchi, K.; Harada, A.; Sugiyam, E.; Harano, K. *Tetrahedron Lett.* **1998**, *39*, 9751–9754.
(7) Yoshitake, Y.; Misaka, J.; Setoguchi, K.; Abe, M.; Kawaji, T.; Eto, M.; Harano, K. *J. Chem. Soc., Perkin Trans. 2* **2002**, 1611–1619.
(8) Cao, H.; Diaz, D. I.; DiCesare, N.; Lakowicz, J. R.; Heagy, M. D. *Org. Lett.* **2002**, *4*, 1503–1505.
(9) Head, N. J.; Oliver, A. M.; Look, K.; Lokan, N. R.; Jones, G. A.; Paddon-Row, M. N. *Angew. Chem., Int. Ed.* **1999**, *38*, 3219–3222.
(10) Tyson, D. S.; Carbaugh, A. D.; Ilhan, F.; Santos-Pérez, J.; Meador, M. A. *Chem. Mater.* **2008**, *20*, 6595–6596.
(11) Grossmann, G.; Potrzebowski, M. J.; Olejniczak, S.; Ziółkowska, N. E.; Bujacz, G. D.; Ciesielski, W.; Prezdo, W.; Nazarov, V.; Golovko, V. *New J. Chem.* **2003**, *27*, 1095–1101.
(12) Carroll, W. R.; Pellechia, P.; Shimizu, K. D. *Org. Lett.* **2008**, *10*, 3547–3550.
(13) Salvati, M. E.; Balog, A.; Wei, D. D.; Pickering, D.; Attar, R. M.; Geng, J.; Rizzo, C. A.; Hunt, J. T.; Gottardis, M. M.; Weinmann, R.; Martinez, R. *Bioorg. Med. Chem. Lett.* **2005**, *15*, 389–393.
(14) Chou, T.-C.; Liao, K.-C.; Lin, J.-J. *Org. Lett.* **2005**, *7*, 4843–4846.

(15) Chou, T.-C.; Hwa, C.-H.; Lin, J.-J.; Liao, K.-C.; Tseng, J.-C. *J. Org. Chem.* **2005**, *70*, 9717–9726.
(16) Mati, L. K.; Cockroft, S. L. *Chem. Soc. Rev.* **2010**, *39*, 4195–4205.
(17) Chein, R.-J.; Corey, E. J. *Org. Lett.* **2010**, *12*, 132–135.
(18) Nishio, M. *CrystEngComm* **2004**, *6*, 130–158.
(19) Kim, E.-i.; Paliwal, S.; Wilcox, C. S. *J. Am. Chem. Soc.* **1998**, *120*, 11192–11193.
(20) Jennings, W. B.; Farrell, B. M.; Malone, J. F. *Acc. Chem. Res.* **2001**, *34*, 885–894.
(21) Tsuzuki, S.; Honda, K.; Uchimaru, T.; Mikami, M.; Tanabe, K. *J. Am. Chem. Soc.* **2002**, *124*, 104–112.
(22) Takaguchi, Y.; Tajima, T.; Yanagimoto, Y.; Tsuboi, S.; Ohta, K.; Motoyoshiya, J.; Aoyama, H. *Org. Lett.* **2003**, *5*, 1677–1679.
(23) Ishida, Y.; Kai, Y.; Kato, S.-Y.; Misawa, A.; Amano, S.; Matsuoka, Y.; Saigo, K. *Angew. Chem., Int. Ed.* **2008**, *47*, 8241–8245.
(24) Four configurational isomers, head-to-head (HH) or head-to-tail (HT) isomers with syn or anti isomerism, are possibly formed from the photodimerization of **1b**. The HH dimers, either syn- or anti-, were not considered in view of steric hindrance that would impede molecules of **1b** to properly align for effective solid-state photodimerization.
(25) When irradiated at the wavelengths below 270 nm (λ_{ex} < 270 nm), all *N*-anthrylsuccinimides and anhydride **6** exhibited very weak fluorescence (Φ_{fl} < 0.001%).
(26) Langhals, H.; Saulich, S. *Chem.—Eur. J.* **2002**, *8*, 5630–5643.
(27) The absorption and emission spectra of *N*-anthrylsuccinimides have not shown significant red- or blue-shifts in solvents of different polarity, indicating the absence of intramolecular charge transfer in these molecular systems.
(28) At relatively lower concentration (1×10^{-6} M), the same activity was also observed, confirming that the fluorescence energy transfer occurs intramolecularly.
(29) Melinger, J. S.; Pan, Y.; Kleiman, V. D.; Peng, Z.; Davis, B. L.; McMorrow, D.; Lu, M. *J. Am. Chem. Soc.* **2002**, *124*, 12002–12012.